

# A MIKE + UVES Survey of Sub-Damped Lyman- $\alpha$ Systems at $z < 1.5$ .

Joseph D. Meiring<sup>1\*</sup>, James T. Lauroesch<sup>1</sup>, Varsha P. Kulkarni<sup>2</sup>, Celine Péroux<sup>3</sup>, Pushpa Khare<sup>4</sup>, & Donald G. York<sup>5,6</sup>

<sup>1</sup>*Department of Physics and Astronomy, University of Louisville, Louisville, Ky 40292 USA*

<sup>2</sup>*Department of Physics and Astronomy, University of South Carolina, Columbia, SC 29208, USA*

<sup>3</sup>*Laboratoire d'Astrophysique de Marseille, OAMP, Université Aix-Marseille & CNRS, 13388 Marseille cedex 13, France*

<sup>4</sup>*Department of Physics, Utkal University, Bhubaneswar, 751004, India*

<sup>5</sup>*Department of Astronomy and Astrophysics, University of Chicago, Chicago, IL 60637, USA*

<sup>6</sup>*Enrico Fermi Institute, University of Chicago, Chicago, IL 60637, USA*

Accepted ... Received ...; in original form ...

## ABSTRACT

We have combined the results from our recent observations of Damped and sub-Damped Lyman- $\alpha$  systems with the MIKE and UVES spectrographs on the Magellan Clay and VLT Kueyen telescopes with ones from the literature to determine the  $N_{\text{H I}}$ -weighted mean metallicity of these systems based both on Fe, a depleted element in QSO absorbers and the local ISM, and Zn a relatively undepleted element. In each case, the  $N_{\text{H I}}$  weighted mean metallicity is higher and shows faster evolution in sub-DLAs than the classical DLA systems. Large grids of photoionisation models over the sub-DLA  $N_{\text{H I}}$  range with CLOUDY show that the ionisation corrections to the abundances are in general small, however the fraction of ionized H can be up to  $\sim 90$  per cent. The individual spectra have been shifted to the rest frame of the absorber and averaged together to determine the average properties of these systems at  $z < 1.5$ . We find that the average abundance pattern of the Sub-DLA systems is similar to the gas in the halo of the Milky Way, with an offset of  $\sim 0.3$  dex in the overall metallicity. Both DLAs and Sub-DLAs show similar characteristics in their relative abundances patterns, although the DLAs have smaller  $\langle [\text{Mn}/\text{Zn}] \rangle$  as well as higher  $\langle [\text{Ti}/\text{Zn}] \rangle$  and  $\langle [\text{Cr}/\text{Zn}] \rangle$ . We calculate the contribution of sub-DLAs to the metal budget of the Universe, and find that the sub-DLA systems at  $z < 1.5$  contain a comoving density of metals  $\Omega_{\text{met}} \sim (3.5\text{-}15.8) \times 10^5 M_{\odot} \text{ Mpc}^{-3}$ , at least twice the comoving density of metals in the DLA systems. The sub-DLAs do however track global chemical evolution models much more closely than do the DLAs, perhaps indicating that they are a less dust biased metallicity indicator of galaxies at high redshifts than the DLA systems.

**Key words:** Quasars: absorption lines-ISM: abundances

## 1 INTRODUCTION

Even with the recent introduction of large telescopes coupled with sensitive instrumentation, studying the properties of distant, high redshift ( $z$ ) galaxies still remains a difficult task. When studied via emission, biases towards more luminous galaxies, i.e. the Malmquist bias, are often present. One of the most fundamental and basic predictions of galaxy evolution models is that the metallicity of the galaxy should

increase over time with the ongoing cycles of star formation and death that pollute the Interstellar Medium (ISM) of the galaxy with heavy elements in successively higher amounts with each subsequent generation of stars.

Chemical evolution studies of the Milky Way are able to utilize individual stellar abundances over a wide range of metallicities to constrain models of the evolution of the Galaxy (see for instance Pagel & Tautvaisiene (1998); Samland (1998); Nissen et al. (2000, 2004)). Direct stellar abundance measurements are difficult in even the most nearby galaxies, and currently impossible at higher redshifts. An opportunity to study the ISM of high redshift galaxies

\* Previous Address: Department of Physics and Astronomy, University of South Carolina, Columbia SC, 29208

occurs if a galaxy is fortuitously aligned along the line of sight to a distant Quasar (QSO), as the gas produces narrow absorption lines in the continuum of the background QSO.

These absorption line systems seen in the spectra of QSOs provide an alternative approach to studying distant galaxies, and offer a unique window into the ISM of high  $z$  galaxies as well as the diffuse Intergalactic Medium (IGM) (see for instance Lehner et al. (2007); Tripp et al. (2008); Danforth & Shull (2008); Frank, Mathur & York (2008) for recent studies of the metal content of the IGM). As these galaxies are not selected upon any morphological criteria, this approach studies galaxies independent of a particular morphological type. The metal ( $Z > 2$ ) abundances in the ISM of these galaxies yield important clues into the processes of star formation and death and the overall chemical enrichment of the system being investigated.

Based upon their neutral hydrogen column densities, intervening absorption line systems with strong Lyman- $\alpha$  lines showing damping wings can be classified into the Damped Lyman- $\alpha$  systems (DLAs with  $\log N_{\text{H I}} \geq 20.3$ ) and sub-DLA systems (sub-DLA  $19 \lesssim \log N_{\text{H I}} < 20.3$ , Péroux et al. 2001). The damping wings which give rise to the name of these systems and can be used to accurately measure  $N_{\text{H I}}$  in these systems begin the sub-DLA regime of  $\log N_{\text{H I}} \sim 19.0$ . With their high gas content, the DLA and sub-DLA systems are expected to be associated directly with galaxies at high redshift, and several systems have been confirmed with followup imaging at lower  $z$  (Le Brun et al. 1997; Bowen, Tripp & Jenkins 2001; Chen et al. 2003).

After much investigation, the DLA systems have been found to have low metallicity ( $\sim 0.15Z_{\odot}$ ) and show little chemical evolution from  $0.1 < z < 3.5$  (Kulkarni et al. 2005, 2007; Meiring et al. 2006; Prochaska et al. 2003; Wolfe, Gawiser & Prochaska 2005). which contradicts galactic chemical evolution models (Pei, Fall, & Hauser 1999; Cen et al. 2003). If the DLAs, which do not appear to contain the metals predicted by chemical evolution models, could these missing metals be hiding in other locations, have they been systematically underestimated in DLAs, or both? This survey was conducted to obtain high resolution spectra in a homogenous sample of the lesser studied sub-DLAs to further investigate their role in cosmic chemical evolution.

The global metal budget of the Universe can be estimated based on the integrated comoving star formation rate density  $\dot{\rho}_{\star}$ , and the theoretical metal production yields of stars ( $\langle p_z \rangle$ ) (Searle & Sargent 1972; Bouché et al. 2008). Adding the contributions from the Lyman- $\alpha$  forest, Lyman break galaxies, sub-mm galaxies, BX/BM galaxies (i.e. Adelberger et al. 2004) and the DLA systems to the global metal budget of the Universe, a dearth of  $\sim 40\%$  of the expected metal content is seen (Bouché, Lehnert & Péroux 2006; Bouché et al. 2008). Several groups have reported high abundances in sub-DLA systems (Khare et al. 2004; Péroux et al. 2006a; Prochaska et al. 2006; Meiring et al. 2007; Srianand et al. 2008; Quast, Reimers & Baade 2008). Strong Lyman- $\alpha$  forest lines with  $\log N_{\text{H I}} \lesssim 16$  have also been recently observed to have super-solar metallicities, although ionisation correction factors are important and not easily constrained (Charlton et al. 2003; Ding et al. 2003; Masiero et al. 2005). It has also been suggested that a large

portion of these missing metals may be locked into the hot intergalactic medium as well (Ferrara et al. 2005).

Although redshifts  $z < 1.5$  span 70% of the age of the Universe (assuming the “737” concordance cosmology of  $\Omega_{\Lambda} = 0.7$ ,  $\Omega_m = 0.3$ ,  $H_0 = 70 \text{ km s}^{-1} \text{ Mpc}^{-1}$  which we utilize throughout this work), few observations have been made of  $z < 1.5$  sub-DLAs due to the lack of spectrographs with enough sensitivity in short wavelengths and the paucity of known sub-DLAs in this redshift range since  $N_{\text{H I}}$  must be determined with space based spectrographs as the Lyman- $\alpha$  line lies in the UV at these redshifts. This range is clearly important for understanding the nature of sub-DLA systems along with galactic chemical evolution.

In this paper we discuss the full sample of sub-DLAs obtained in this survey with the Magellan-II telescope and the MIKE spectrograph and the VLT Kuyuen telescope with the UVES spectrograph. The structure of this paper is as follows. In § 2 we discuss details of our sample. In § 3, we discuss the abundances and column density determinations. § 4 gives information on photoionisation models with CLOUDY. In § 5 we discuss the kinematical properties of these systems. In § 6 we give the  $N_{\text{H I}}$ -weighted mean metallicity based on both Fe and Zn. We discuss the averaged sub-DLA spectrum in § 7. In § 8 we estimate the contribution of sub-DLA systems to the comoving metal budget, and in § 9 we discuss the implications of these measurements.

## 2 SAMPLE SELECTION

The observations in this sample were made with the 6.5m Magellan-II Clay telescope and the Magellan Inamori Kyocera Echelle (MIKE) spectrograph (see Bernstein et al. 2003) along with the 8.2m Very Large Telescope (VLT) Kuyuen telescope with the Ultraviolet Visual Echelle Spectrograph (UVES, see D’Odorico et al. 2000 for details of the instrument). These observations were undertaken from 2005 until 2008. Our total sample includes spectra of 27 QSOs and a total of 34 systems, with 31 sub-DLAs or strong Lyman-limit systems and three DLAs. These results have been published in Meiring et al. (2007, 2008, 2009) and Péroux et al. (2008).

Our targets were selected from the Rao, Turnshek, & Nestor (2006) catalog of *Mg II absorbers* identified in Hubble Space Telescope (HST) spectra having  $0.65 \lesssim z_{\text{abs}} \lesssim 1.5$  (so that the Zn II  $\lambda\lambda 2026, 2062$  lines were redshifted into the optical) with  $19.0 \lesssim N_{\text{H I}} < 20.3$ . Due to the lower H I column densities and hence lower expected Zn II column densities for sub-solar metallicity systems in the  $N_{\text{H I}}$  range, we required the background QSO to be brighter than  $m_g \lesssim 18.5$  in order to achieve S/N ratios adequate to detect the expected weak Zn II lines.

Ideally, a blind survey of QSOs is the best possible option with minimal bias. This is however unfeasible due to the necessity of both ground and space based spectra, and the small coincidence rate of Sub-DLAs or DLAs in the spectra of background QSOs. An Mg II selection criterion is not likely to significantly bias the sample, as the rest frame equivalent width of the Mg II  $\lambda\lambda 2796, 2803$  lines does not correlate well with  $[\text{Zn}/\text{H}]$  or  $[\text{Fe}/\text{H}]$  for DLAs or sub-DLAs. (Kulkarni et al. 2007; Dessauges-Zavadsky, Ellison, & Murphy 2009). Of the  $\sim 45$

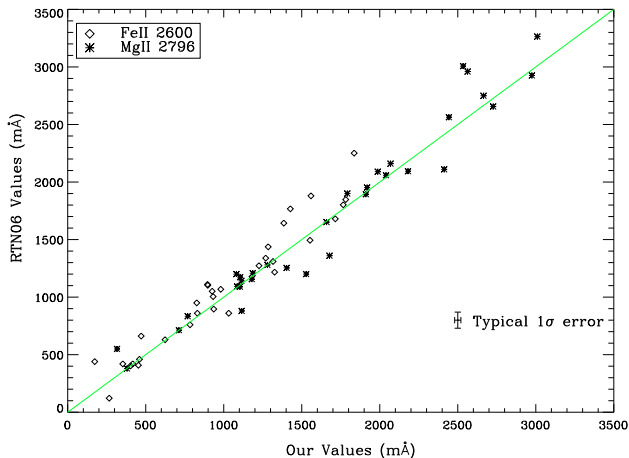


**Figure 1.** A comparison of the rest frame equivalent widths of Mg II  $\lambda$  2796 and Fe II  $\lambda$  2600 from these data, and from the lower resolution spectra from Rao, Turnshek, & Nestor (2006).

systems from the Rao, Turnshek, & Nestor (2006) sample, only eight systems remain at  $z \lesssim 1.5$  that fit the selection criteria above and not observed in the sample presented here due to scheduling and time constraints. These objects have similar mean  $W_0^{2796}$  ( $\sim 1.4$  Å compared to  $\sim 1.6$  Å for systems that we have observed), and thus are unlikely to bias the sample.

Throughout this paper the QSO names are given in J2000 coordinates. We show a comparison of the rest frame equivalent widths as measured by Rao, Turnshek, & Nestor (2006) and the values determined in these higher resolution spectra for the Mg II  $\lambda$  2796 and Fe II  $\lambda$  2600 lines in Figure 1. The values appear to be in excellent agreement, with no systematic differences in the two measurements.

### 3 ABUNDANCES

Total abundances for the observed systems are given in Table 3. These values have been given in our previous works (see Meiring et al. 2007, 2008, 2009; Péroux et al. 2006b), and are compiled here for completeness and convenience to the reader. We have used the total column densities (i.e. the sum of the column densities in the individual components of a system that were determined via profile fitting method) along with the total  $N_{\text{H I}}$  as given in Table 3, to determine the abundances of these systems. We have not placed any ionisation corrections while determining these abundances (the issue of ionisation corrections is discussed further in Section 4), and have assumed the first ions to be the dominant ionisation species of the elements for which these abundances have been determined, namely Zn, Fe, Mn, Cr, and Si. Solar systems abundances from Lodders (2003) are also given in Table 3.

In Table 3, we have given the metallicities of Zn and Fe, the relative abundances of a several species, as well as the column density ratios of adjacent ions of a few elements. All these are based on the column densities obtained from the profile fitting analysis. Relative abundances like  $[\text{Zn}/\text{Fe}]$ , are indicators of dust depletion, and ion ratios like Al II/Al

III, may provide information about the ionization in the systems.

### 4 PHOTOIONISATION MODELS

The gas in DLA systems is expected to remain largely neutral due to self-shielding of the UV photons capable of ionization. The ionisation correction factor, defined here as

$$\epsilon = [X/H]_{\text{total}} - [X^+/H^0] \quad (1)$$

where the total column densities include contributions from all ionisation stages, has been investigated for DLAs by several groups (Howk & Sembach 1999; Vladilo et al. 2001; Prochaska et al. 2002). The ionisation corrections for most elements in DLA systems were found to be  $\lesssim 0.2$  dex in most cases. Due to the lesser amount of H I in the sub-DLA systems, and hence less shielding, it is expected that they should show a greater amount of ionisation.

It has previously been shown that the ionisation corrections based on CLOUDY models are in general also expected to be small for sub-DLA systems (Dessauges-Zavadsky et al. 2003; Meiring et al. 2007, 2008). Here, we expand upon our previous CLOUDY modeling with grids of photoionisation models over the entire sub-DLA  $N_{\text{H I}}$  range. Models were created with version C06.02.b of CLOUDY, last described by Ferland et al. (1998). Grids of CLOUDY models were computed assuming that the spectrum of ionizing radiation striking the cloud followed the form of the extra-galactic UV background of Haardt & Madau (Haardt & Madau 1996; Madau, Haardt, & Rees 1999) at the appropriate redshift of the absorber, plus the model stellar atmosphere of Kurucz with a temperature of 30,000K to simulate a radiation field produced via an O/B-type star. Both radiation fields were combined in equal parts for the final incident spectrum. Plots of both types of spectra can be found in Hazy, the documentation for CLOUDY which can be found at [\protect\vrulewidth0pthttp://www.nublado.org](http://www.nublado.org). In addition, our CLOUDY models have included a cosmic ray background and cosmic microwave background. These simulations however do not include radiation from local shocks caused by supernovae, or compact sources such as white dwarfs or compact binary systems, all of which likely contribute the ionizing radiation field.

For each of the grids of models, the ionisation parameter defined by

$$U = \frac{n_\gamma}{n_{\text{H}}} = \frac{\Phi_{912}}{cn_{\text{H}}} \quad (2)$$

(where  $\Phi_{912}$  is the flux of radiation with  $h\nu > 13.6$  eV) was increased from  $\log U = -6.0$  to 0.

Results for the ionisation corrections for Fe and Si are shown in Figures 2 and 3 as a function of  $N_{\text{H I}}$  and  $\log U$ . As defined above, for a ratio  $X^+/H^0$  one must add  $\epsilon$  to get the true abundance  $X/H$ . Fe appears unaffected except in the extreme case of low  $N_{\text{H I}}$  and high ionisation parameter  $U$ . As was noted in Dessauges-Zavadsky et al. (2003) and Meiring et al. (2007, 2008) in all cases where a constraint on the ionization parameter could be placed in the modeled sub-DLA systems,  $\log U \lesssim -2.5$ , indicating that the correction factors are at most  $\sim -0.2$  dex, in the sense that the measured abundances may be slightly higher than the true

QSO	$z_{abs}$	$\log N_{\text{H I}}$	[Zn/H]	[Fe/H]	[Fe/Zn]	[Si/Fe]	[Ca/Fe]	[Cr/Fe]	[Mn/Fe]	Al III / Al II	Mg II / Mg I	Mg II / Al III	Fe II / Al III	$\Delta v_{90}$
[X/Y] $_{\odot}$			-7.37	-4.53	+2.84	+0.07	-1.13	-1.82	-1.97					km s $^{-1}$
Q0005+0524	0.8514	19.08±0.04	< -0.47	-0.76±0.05	> -0.29	-	-	< -0.09	< -0.81	-	>2.14	>+1.21	0.68±0.04	39
Q0012-0122	1.3862	20.26±0.02	< -1.34	-1.49±0.03	> -0.15	+0.12±0.08	-	< -0.53	< -0.86	< -0.19	>2.36	>+1.20	1.35±0.03	32
Q0021+0104	1.3259	20.04±0.11	< -1.19	-0.82±0.11	> +0.37	>+0.14	-	< -0.66	< -0.85	-	>2.70	-	-	185
Q0123-0058	1.4094	20.08±0.09	-0.45±0.20	-0.55±0.12	-0.10±0.11	+0.42±0.06	-	-0.25 ± 0.10	-0.40 ± 0.12	-	-	-	1.22±0.03	140
Q0132+0116	1.2712	19.70±0.09	< -0.54	-0.53±0.12	> +0.01	-	-	< -0.67	< -1.10	-	-	-	1.04±0.02	207
Q0138-0005	0.7821	19.81±0.09	+0.28±0.16	> -0.09	> -0.37	-	-	-	-	-	>2.91	-	-	95
Q0153+0009	0.7714	19.70±0.09	< -0.34	-	-	-	-	-	-	-	>2.88	>+3.16	-	278
Q0354-2724	1.4051	20.18±0.15	-0.08±0.16	-0.50±0.16	-0.43±0.06	-	-	+0.02±0.07	-0.28±0.08	<-0.79	>2.36	>1.67	1.74±0.06	176
Q0427-1302	1.4080	19.04±0.04	< -0.58	-1.15±0.04	> -0.57	+0.16±0.03	-	<+0.33	<+0.26	< -1.14	-	-	>2.30	42
Q0826-2230	0.9110	19.04±0.04	+0.68±0.08	-0.94±0.06	-1.63±0.08	<+0.58	-0.69±0.07	<+0.36	< -0.23	-	>1.67	>2.04	>1.85	276
Q1009-0026A	0.8426	20.20±0.06	< -0.98	-1.28±0.07	> -0.31	-	-	< -0.16	-0.16±0.06	-	>2.57	>1.57	1.66±0.06	36
Q1009-0026B	0.8866	19.48±0.05	+0.25±0.06	-0.58±0.06	-0.83±0.06	< -0.18	-0.98±0.06	< -0.44	-0.05±0.08	-	>2.11	>1.40	1.25±0.05	94
Q1010-0047	1.3270	19.81±0.05	< -0.75	-0.75±0.06	> +0.01	+0.42±0.07	-	< -0.34	< -0.71	< -0.71	>2.71	>1.69	1.25±0.05	156
Q1037+0028	1.4244	20.04±0.12	< -0.63	-0.67±0.12	> -0.04	+0.18±0.04	-	< -0.76	-0.34±0.05	< -0.96	-	>2.29	1.65±0.03	169
Q1054-0020A	0.8301	18.95±0.18	< +0.18	-0.09±0.18	> -0.28	-	-	< -0.04	-0.09±0.07	-	>2.28	>1.24	0.74±0.06	85
Q1054-0020B	0.9514	19.28±0.02	< -0.21	-1.09±0.02	> -0.88	< +0.52	-	< +0.36	< +0.23	-	>1.68	>1.61	>1.55	160
Q1215-0034	1.5543	19.56±0.02	< -0.56	-0.64±0.02	> -0.08	-	-	< -0.20	< -0.79	-	-	>2.57	1.62±0.03	81
Q1220-0040	0.9746	20.20±0.07	< -1.14	-1.33±0.07	> -0.19	-	-	< -0.14	< -0.42	-	>2.69	>2.19	1.72±0.06	95
Q1224+0037	1.2665	20.00±0.07	< -0.78	-0.93±0.11	> -0.16	< -0.31	-	< -0.35	< -0.41	< -0.74	>2.97	>1.99	1.56±0.12	280
Q1228+1018	0.9376	19.41±0.02	< -0.37	-0.30±0.02	> +0.07	-	-	< -0.55	< -0.47	-	>2.29	>1.51	1.48±0.10	116
Q1330-2056	0.8526	19.40±0.02	< -0.07	-1.07±0.02	> -1.00	-	-	< +0.20	< -0.22	-	>1.88	>1.62	1.21±0.05	578
Q1436-0051A	0.7377	20.08±0.11	-0.05±0.12	-0.61±0.11	-0.58±0.04	-	-0.98±0.03	< -0.41	+0.04±0.03	-	-	-	-	71
Q1436-0051B	0.9281	<18.8	>+0.86	> -0.07	-0.94±0.06	+0.75±0.05	-0.79±0.04	< +0.20	+0.22±0.05	-	>2.63	>1.72	0.80±0.03	62
Q1455-0045	1.0929	20.08±0.06	< -0.80	-0.98±0.06	> -0.18	+0.00±0.10	-	-0.35±0.13	-0.51±0.15	< -0.18	>2.39	>1.27	0.92±0.02	121
Q1631+1156	0.9004	19.70±0.04	< -0.15	-1.06±0.06	> -0.91	-	-0.85±0.07	<+0.36	<+0.40	-	>1.83	-	-	58
Q2051+1950	1.1157	20.00±0.15	+0.27±0.18	-0.45±0.15	-0.72±0.10	+0.06±0.07	-1.34±0.04	-0.31±0.10	+0.16±0.03	< -0.17	>1.97	>+1.08	1.49±0.04	113
Q2331+0038	1.1414	20.00±0.05	-0.51±0.12	-1.09±0.06	-0.59±0.11	< -0.12	-	< -0.19	< -0.62	< -0.40	>2.31	>1.77	1.36±0.09	137
Q2335+1501	0.6798	19.70±0.30	+0.07±0.34	-0.32±0.33	-0.39±0.05	-	-1.29±0.04	-0.12 ± 0.11	-	-	>2.77	-	-	95
Q2352-0028A	0.8730	19.18±0.09	< -0.14	-1.17±0.09	> -1.03	-	-	<+0.71	< -0.05	-	>2.42	-	-	120
Q2352-0028B	1.0318	19.81±0.13	< -0.51	-0.37±0.13	> +0.14	+0.51±0.03	-	-0.13±0.06	< -1.07	-	>2.41	>+1.53	1.50±0.03	164
Q2352-0028C	1.2467	19.60±0.24	< -0.7	-0.86±0.24	> -0.16	-	-	< -0.22	< -0.64	< -0.10	>2.91	>+1.85	0.82±0.03	240

**Table 1:** Elemental abundances and adjacent ion ratios for the absorbers in this sample. The solar abundances from Lodders (2003) are given in the headings as well. In the last four columns, the ratios of the column densities of several pairs of ions are given in dex.  $N_{\text{H I}}$  is given in logarithmic form in units of  $\text{cm}^{-2}$ .

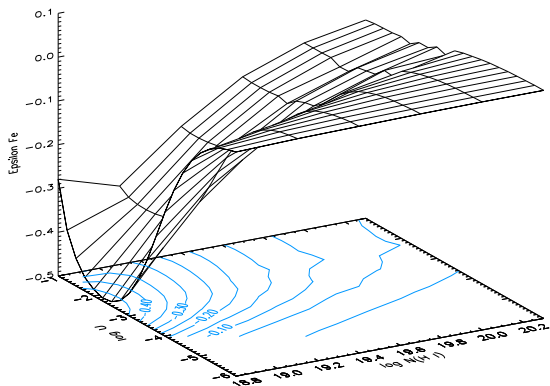


**Figure 2.** Results of the CLOUDY photoionisation models for the ionisation correction needed for Fe as a function of  $\log U$  and  $N_{\text{H I}}$ . The blue contours on the horizontal plane represent the ionisation corrections in steps of 0.05 dex.

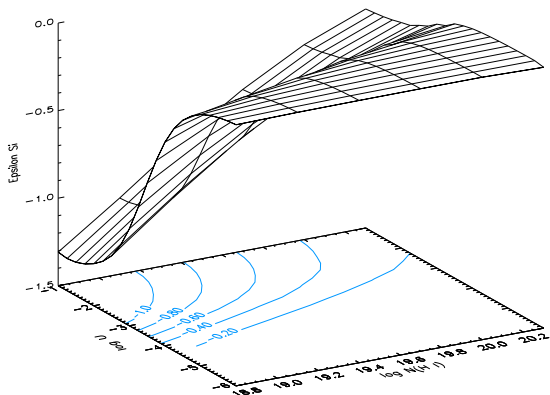


**Figure 3.** Results of the CLOUDY photoionisation models for the ionisation correction needed for Si as a function of  $\log U$  and  $N_{\text{H I}}$ . The blue contours on the horizontal plane represent the ionisation corrections in steps of 0.20 dex.

abundances. With low ionisation parameters  $U$ ,  $\text{Fe}^+/\text{Si}^+$  is an accurate indicator of  $\text{Fe}/\text{Si}$ , however at higher ionisation parameters ( $\log U \gtrsim -2$ ),  $\text{Fe}^+/\text{Si}^+$  is higher than the true  $\text{Fe}/\text{Si}$ , mimicking the effects of differential and higher depletion of Fe than Si.

We have also investigated the fractional ionisation of hydrogen in these sub-DLA systems to determine the overall levels of ionisation which are needed to determine the contribution of sub-DLAs to the global metallicity. These simulations are more reliable than simulations of the ionisation of the metal species due to the direct calculability of the atomic properties of hydrogen such as the recombination rates, ionisation cross sections, and oscillator strengths. Again, we assumed a hot stellar spectrum with  $T = 30,000$  K, and the diffuse extragalactic background from AGN and starburst galaxies at  $z \sim 1$ . Constant density was assumed with  $n = 1$  atom  $\text{cm}^{-3}$ . Starting with  $\log N_{\text{H I}} = 18.8$ , the column density was increased by 0.2 dex in each subsequent iteration. Three separate ionisation parameters were

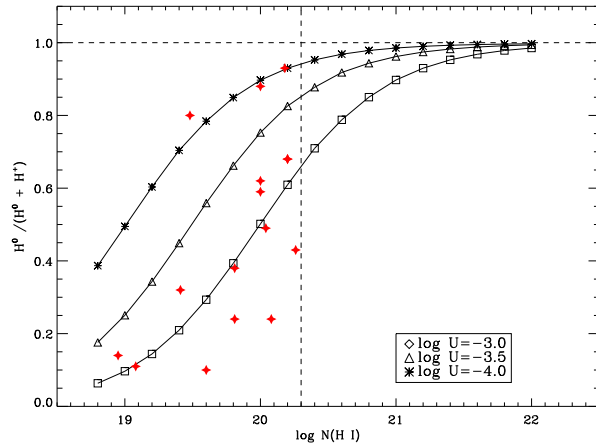


**Figure 4.** Results of the CLOUDY photoionisation models for the ionisation of hydrogen in these sub-DLA systems. The neutral fraction,  $H^0/(H^0 + H^+)$  is plotted on the y axis, with  $\log N_{\text{H I}}$  along the abscissa. Also plotted as red stars are the ionisation fractions derived from CLOUDY models of each individual system.

used, with values of  $\log U = -4.0$ ,  $-3.5$ , and  $-3.0$ . These values were chosen because the sub-DLAs in this sample and Dessauges-Zavadsky et al. (2003); Péroux et al. (2007) all seem to have values of the ionisation parameter in or below this range. Results of the simulations are shown in Figure 4. Overplotted in the figure are the values for the ionisation parameters derived from individual CLOUDY models for the systems in this sample.

In general, the sub-DLAs contain large fractions of ionized gas based upon these simulations, especially the systems with the lowest  $N_{\text{H I}}$  while the DLAs are largely neutral in H. This was also reported for higher  $z$  systems by (Péroux et al. 2007). However, for a given  $N_{\text{H I}}$  a large range of ionisation fractions are seen, perhaps indicating that there are several types of environments from which the sub-DLAs are being drawn.

There are several unknowns however. The shape of the ionizing radiation field does affect the overall ionisation. The Haardt & Madau background spectrum is a theoretical construct, and has not been accurately tested and as such is only one of many possibilities. The hot stellar spectrum used in these simulations, although certainly measurable in the Milky Way, may also not accurately reflect the true radiation field incident on these systems.

## 5 KINEMATICS OF SUB-DLAs

Following the analysis of Ledoux et al. (2006), we performed an analysis of the apparent optical depth (see e.g., Savage & Sembach 1996) of these sub-DLA systems. The apparent optical depth is defined as

$$\tau(\lambda)_a = \ln[I_0(\lambda)/I_{\text{obs}}(\lambda)] \quad (3)$$

where  $I_0(\lambda)$  is the continuum level, and  $I_{\text{obs}}(\lambda)$  is the observed intensity. Specifically, we integrated the AOD profile over the extent of the line, and give the velocity width ( $\Delta v_{90}$ )

as the value where the inner 90 percent of the absorption occurs.

In Figure 5 the metallicity vs  $\Delta v_{90}$  for the systems in Ledoux et al. (2006); Péroux et al. (2006b, 2008); Prochaska et al. (2006); Noterdaeme et al. (2008a); Quast, Reimers & Baade (2008) as well as the systems from this work. In their analysis, Ledoux et al. (2006) used absorption features where 40 to 90 percent of the continuum level was absorbed by the line. We have tried to follow this strategy whenever possible for these systems. For most systems, the Fe II  $\lambda$  2374 line was used in the velocity width determination, as it is typically unsaturated in these systems, and also strong enough to include absorption from weaker features. For systems where the Fe II  $\lambda$  2374 feature was too weak, the Fe II  $\lambda$  2344 feature was typically used. From the Ledoux et al. (2006) sample, we have only included the Zn, and not the Si and S detections in Figure 5.

The non-parametric Wilcoxon Rank-Sum test was used to determine if the populations of sub-DLAs and DLAs were distinct in their mean velocity widths. The test statistic  $Z$  describing the significance of the difference in the means of the two populations was determined to be  $Z = 0.94$ , with a probability of the sample populations having the same mean of 17 per cent. Similarly, a Kolmogorov-Smirnov test shows that the populations of DLA and sub-DLA velocity widths having the same mean is  $\sim 18$  per cent. The non-parametric approach used here is more appropriate than a two sample t-test, as we do not know the underlying distributions of the kinematics of these populations. A similar weak discrepancy was also seen by Zwaan et al. (2008), wherein the lower column density systems also had slightly larger  $\Delta v_{90}$  values.

As can be seen in Figure 5, the DLAs do show a fairly tight correlation between their metallicities and velocity widths. Interestingly, the sub-DLAs however do not show this trend. The Kendall's  $\tau$  test was used for both the DLAs and sub-DLAs to test for a correlation between the metallicity and velocity width. For the DLAs, a clear correlation is present with  $\tau = 0.59$  and a probability of no correlation  $p < 0.001$ . Conversely, the sub-DLAs show no evidence of correlation with  $\tau = 0.09$  and a probability of no correlation of  $p \sim 60$  percent. This however is possibly due to a lack of Zn detections at low  $[Zn/H]$ .

## 6 $N_{\text{H I}}$ -WEIGHTED MEAN METALLICITY

### 6.1 $[\text{Fe}/\text{H}]$ Metallicity Evolution

The  $N_{\text{H I}}$ -weighted mean metallicity given by:

$$\langle [X/H] \rangle = \log \langle (X/H) \rangle - \log (X/H)_{\odot} \quad (4)$$

where

$$\langle (X/H) \rangle = \frac{\sum_{i=1}^n N(X)_i}{\sum_{i=1}^n N(H)_i} \quad (5)$$

with the errors estimated by the standard deviation,

$$\sigma^2 = \left[ \sum_{i=1}^n w_i ([X/H]_i - \langle [X/H] \rangle)^2 \right] / (n - 1) \quad (6)$$

and the weights proportional to  $N_{\text{H I}}$  as given by

$$w_i = \frac{N(H)_i}{\sum_{k=1}^n N(H)_k} \quad (7)$$

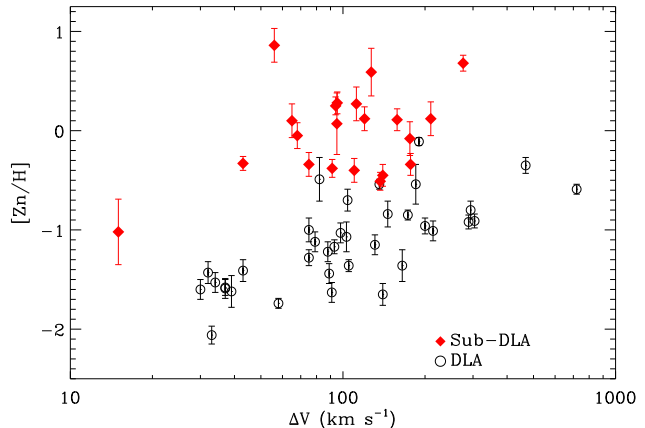


**Figure 5.** The metallicity as measured by the undepleted elements Zn and S vs the velocity width  $\Delta v_{90}$  defined above.

has often been used as a quantitative way of estimating the amount of metal enrichment in the Universe in a given epoch (Péroux et al. 2003b; Kulkarni et al. 2005, 2007). The  $N_{\text{H I}}$ -Weighted Mean Metallicity is thus a measure of the global or average chemical enrichment of the Universe in a given epoch or redshift interval.

As the lines of Fe are comparatively easier to detect and the cosmic abundance of Fe is substantially higher than that of the weaker Fe peak element Zn, Fe abundances for nearly every DLA and sub-DLA observed to date have been determined. There are also multiple lines of Fe II from  $\sim 1200$  to  $\sim 2600$  Å, allowing the possibility for higher redshift systems to be studied, where the Zn II  $\lambda\lambda$  2026, 2062 lines would redshifted out of the visible range. On the other hand, as was previously mentioned, Fe is refractory and is typically depleted onto dust grains.  $[\text{Fe}/\text{H}]$  is therefore a lower limit to the true abundance.

The  $N_{\text{H I}}$ -weighted mean metallicity based on Fe is shown in Figure 6. Sub-DLAs have been plotted as green squares, and DLAs as blue circles. These data were binned into five sub-samples of constant redshift size ( $\Delta z \sim 1$  and solid points) and into bins with roughly equal numbers of systems (open points). Independent of the binning type used, the sub-DLAs do appear to have a faster evolving metallicity, and are generally more metal rich in each redshift interval. Also shown in Figure 6 are the chemical evolution models of Pagel & Tautvaisiene (1998) for the SMC (solid red line), and Pei, Fall, & Hauser (1999) (dashed magenta line) for the global metallicity evolution of the Universe. Both types of models are sophisticated open box analytical models, with the models of Pei, Fall, & Hauser (1999) being averaged over several comoving Mpc to contain multiple galaxies.

### 6.2 $[\text{Zn}/\text{H}]$ Metallicity Evolution and Survival Analysis

Although far easier to detect in QSO absorbers, Fe suffers as a metallicity indicator due to dust depletion. The non-refractory elements of O, S, and Zn are much more reliable indicators of the true metallicity of the system. The O and

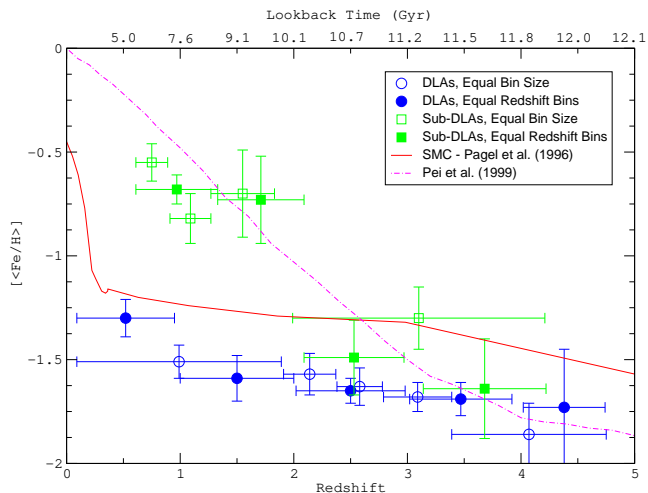


**Figure 6.** The  $N_{\text{H I}}$  weighted mean metallicity for sub-DLAs (green squares) and DLAs (blue circles). Overlaid is the theoretical chemical evolution model from the Pei, Fall, & Hauser (1999) model for the global metallicity (dashed line), and the chemical evolution model of the SMC from Pagel & Tautvaišienė (1998) (solid line). The lookback time in Gyr is given on the upper x axis.

S lines however lie far in the UV, at  $\lambda \sim 1300$  and  $1250 \text{ \AA}$  respectively and are inaccessible without space based observations at  $z \lesssim 2.0$ . The Zn II  $\lambda\lambda 2026, 2062$  lines however are accessible with ground based observations for these systems. The nucleosynthetic origins of Zn are still somewhat a matter of debate. With  $Z=30$ , Zn is not quite a true Fe peak element. The exact production site of Zn is still in question (see for instance the discussion in Mishenina et al. 2002).

The Kaplan-Meier estimator has become the standard non-parametric statistical analysis for dealing with censored data (Kaplan & Meier 1958). The Kaplan-Meier estimator works with any underlying distribution of the data, which is advantageous in the case of this data set for which the underlying distribution of metallicities at a given redshift or redshift interval is not known. We have used the ASURV package provided by the Astrostatistics Center at Penn State University (`protect\vrulewidth0pthttp://astrostatistics.psu.edu`) for determining the summary statistics of the metallicities as measured by  $[\text{Zn}/\text{H}]$  for the DLAs and sub DLAs in this sample and the literature. The details of the package are described in Feigelson & Nelson (1985), for univariate data.

The sub-DLA sample was separated into four bins with (roughly) equal numbers of systems in each bin, with the same done for the DLA systems from the literature along with the two DLAs from these observations. The DLAs were separated into five bins due to the larger sample size. A plot of the metallicity as determined via this survival analysis is shown in Figure 7. The vertical error bars denote the estimate of the variance in each redshift bin, and the horizontal bars denote the range of redshifts in each bin. Errors for the metallicity via survival analysis include only the statistical uncertainty and not any measurement uncertainties. As can be seen in both Figures 7 and 6, the metallicity based on Fe and Zn is faster evolving for the sub-DLA sample than the DLA sample. At  $z \lesssim 1.25$ , the sub-DLA metallicities are  $\sim 0.7$  dex higher than the DLA systems.

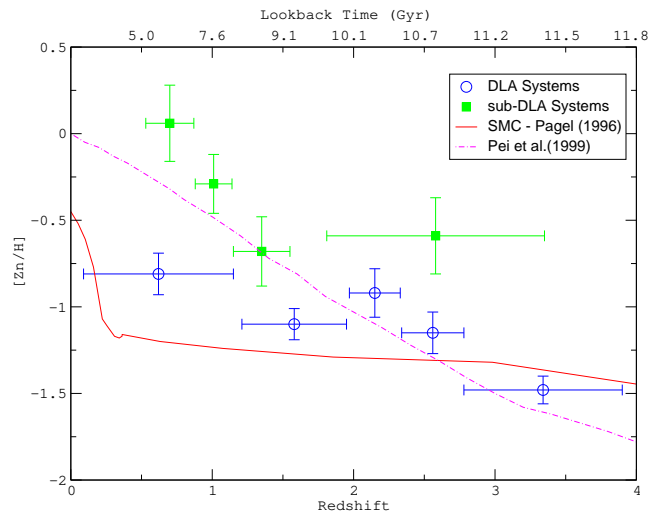


**Figure 7.** The metallicity via survival analysis taking into account upper limits for sub-DLAs (green squares) and DLAs (blue circles). Overlaid is the theoretical chemical evolution model from the Pei, Fall, & Hauser (1999) model for the global metallicity (dashed line), and the chemical evolution model of the SMC from Pagel & Tautvaišienė (1998) (solid line). The lookback time in Gyr is given on the upper x axis

## 7 AVERAGE SUB-DLA SPECTRUM

York et al. (2006) used a sample of  $\sim 800$  lower resolution ( $\sim 2000$ ) SDSS spectra to determine abundances and depletion levels in QSO absorbers by averaging the spectra after shifting them to the rest frame of the absorbers. Weaker absorptions, not seen or seen at lower significance in the individual SDSS spectra, were clearly detected in this average spectrum owing to its higher S/N ratio. Following in the spirit of that work, we have also averaged the spectra of these sub-DLAs.

To determine average abundances of Cr, Fe, Mn, Si, and Ti of the absorbers in this sample, the spectra were shifted to rest wavelengths and averaged. Specifically, the Si II  $\lambda 1808$ , Cr II  $\lambda 2056$ , Fe II  $\lambda\lambda 2260, 2374$  and Zn II  $\lambda 2026$  lines were used. Any obvious non-associated features in the region around the lines of interest in the individual spectra were replaced by Gaussian noise with S/N similar to the uncontaminated regions. For Q0251+1950, a systematic shift of  $\sim 60 \text{ km s}^{-1}$  was applied to the spectra as the redshift reported in Rao, Turnshek, & Nestor (2006) was slightly off. All other spectra were left unaltered. We show the averaged spectra of these transitions in Figure 8.

Column densities for these elements were determined via the AOD method. The profile fitting method, although more robust and generally more accurate can not be used in this case, as the individual components are blended together in the averaged spectra. Rest frame equivalent widths were also determined, with the errors estimated by both photon noise and uncertainties in the continuum placement. Absolute abundances were determined by averaging  $N_{\text{H I}}$  for the systems that were included in the averaged metal line spectrum, while excluding the systems which were not used in the average. Table 2 gives  $W_0$ , the measured column density and corresponding abundance. Interestingly, the metallicity based on Zn from this averaged spectrum matches nearly

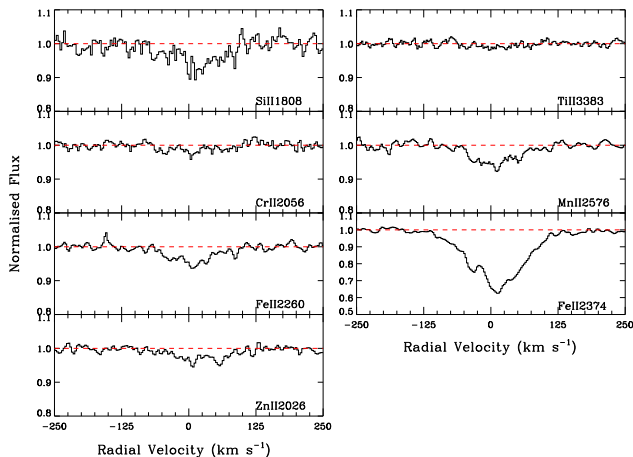


**Figure 8.** The average spectra of the systems in this sample. The key lines of Si II, Fe II, Zn II, Cr II, Mn II are shown here.

**Table 2.** Equivalent widths, abundances and column densities of the averaged spectra.

Transition	# Systems	$W_0$ mÅ	$\log N$ cm <sup>-2</sup>	[X/H] Dex
Si II 1808	15	44±9	14.87±0.08	-0.52 ± 0.08
Ti II 3383	15	12±4	11.52±0.17	-1.14 ± 0.17
Cr II 2056	29	15±4	12.59±0.12	-0.91 ± 0.12
Mn II 2576	25	51±8	12.39±0.06	-0.98 ± 0.06
Fe II 2260	29	37±5	14.53±0.06	-0.79 ± 0.06
Fe II 2374	28	327±7	14.38±0.01	-0.93 ± 0.03
Zn II 2026	31	28±5	12.10±0.08 <sup>a</sup>	-0.38 ± 0.08 <sup>a</sup>

<sup>a</sup>Based on the average column density determined with and without the feature at  $\sim +60$  km s<sup>-1</sup>, which could be due to a contribution from Mg I 2026.

perfectly with the  $N_{\text{H I}}$ -weighted mean metallicity from §6, validating the technique.

The abundance patterns seen in the ISM of the Milky Way, SMC, and DLAs are shown in Figure 9. Abundances from the ISM of the SMC are from Welty et al. (1997) with abundances from the DLAs from (Prochaska & Wolfe 2002). Several points come to light based on the depletion patterns and abundances of these samples. The ISM Si abundance is nearly identical in all three cases. Secondly, the Zn abundance of the averaged sub-DLA spectra lies between the SMC and warm Galactic ISM value. Lastly, the Fe and Cr abundances in the averaged sub-DLA spectra are somewhat higher ( $\sim +0.5$  and  $\sim +0.3$  dex for Fe and Cr respectively) than what is observed in the warm neutral ISM of the Milky Way and SMC.

As the abundance patterns seen in the ISM are closely related to the past star formation rate and history of the galaxy, does the average abundance pattern in sub-DLAs mimic the patterns seen in the Milky Way or ISM, or neither? The SMC and Milky Way have had very different star formation histories, and thus have different elemental abundances. The star formation history of the SMC has recently been investigated by Harris & Zaritsky (2004) based on deep

photometric surveys of the entire SMC. They find that most of the stars in the SMC formed  $\gtrsim 8.5$  Gyr ago (corresponding to redshift  $z \gtrsim 1.2$ ) with a period of quiescence lasting  $\sim 3$  Gyr, followed by more recent bursts in star formation. Tidal interactions with the Milky Way likely play a roll in causing star formation bursts in the SMC (Harris & Zaritsky 2004). The Milky Way has also gone through bursts of star formation, creating the halo and thick disk. The Milky Way however does not appear to have undergone the same long duration periods of quiescence that the SMC underwent, but instead has seemed to continuously form stars (Gilmore 2001; Rocah-Pinto et al. 2000). Sub-DLAs may trace a population of galaxies dissimilar to massive spirals (i.e. the Milky Way) or lower mass irregulars (i.e. the SMC) and thus may have different abundance patterns.

Based upon the average abundance pattern in these sub-DLA systems, it appears as though these systems are more closely related to the Milky Way halo type interstellar medium than the warm neutral ISM of the Milky Way. The Zn metallicity in sub-DLAs,  $[\text{Zn}/\text{H}]$ , as measured in the averaged spectra lies between the values seen in the warm neutral ISM and SMC.  $[\text{Zn}/\text{H}]$  is  $\sim 0.2$  dex less than that of the warm Milky Way ISM and 0.3 dex higher than the SMC. This however reflects  $[\text{Zn}/\text{H}]$  at  $z \sim 1.1$ , the average redshift of these systems. This metallicity is well within the range of values at this redshift from the chemical evolution models mentioned above. The abundance and depletion pattern of the sub-DLAs does very closely resemble that of the halo of the Milky Way, as can be seen in Figure 10.

## 8 THE CONTRIBUTION OF SUB-DLAs TO THE METAL BUDGET OF THE UNIVERSE

It has now been well established that the DLA systems observed to date are metal poor at all redshifts, and show weak evolution with redshift (Kulkarni et al. 2005; Prochaska & Wolfe 2002; Meiring et al. 2006). Including the contributions from star forming Lyman-break galaxies at  $z \sim 2$ , DLAs, and the Lyman- $\alpha$  forest the observations account for only  $\sim 60\%$  of the amount of metals that are expected from the cosmic star formation history (Bouché et al. 2008). Here, we discuss the contribution of the less studied sub-DLA systems to the metal budget of the Universe. For a previous estimation of the comoving metal density in sub-DLAs based on the preliminary results of this work and the literature sample of sub-DLAs, see Kulkarni et al. (2007).

We can estimate the comoving metal density in DLAs and sub-DLAs based on the column density distribution function, metallicities, and in the case of sub-DLAs the ionisation fraction. As was discussed previously, and can be seen in Figure 4, the ionisation fraction in the DLA systems with  $\log N_{\text{H I}} > 20.3$  is negligible, and they can be considered completely neutral to good approximation in the H I phase. See however Wolfe and Prochaska (2000) for a discussion on the more highly ionized gas in DLAs.

The DLAs are well sampled, especially at  $z > 1.5$ , and have a mean metallicity of  $[\text{Zn}/\text{H}] \sim -1.0$  from a robust sample of  $\sim 100$  systems (Prochaska & Wolfe 2002; Kulkarni et al. 2005; Meiring et al. 2006). Using the solar metallicity by mass as determined by Lodders (2003) of  $Z_{\odot} = 0.0177$ , the DLAs thus have a metallicity by mass of  $Z_{\text{DLA}} = 0.00177$ .



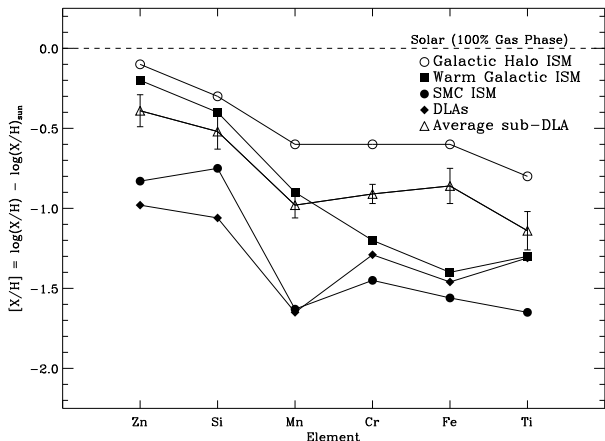


**Figure 9.** The depletion pattern or abundances derived from the averaged sub-DLA spectra of the systems in this sample. Overplotted are the abundances of the Milky Way warm neutral ISM, Milky Way halo, ISM abundances in the SMC, and DLA abundances.

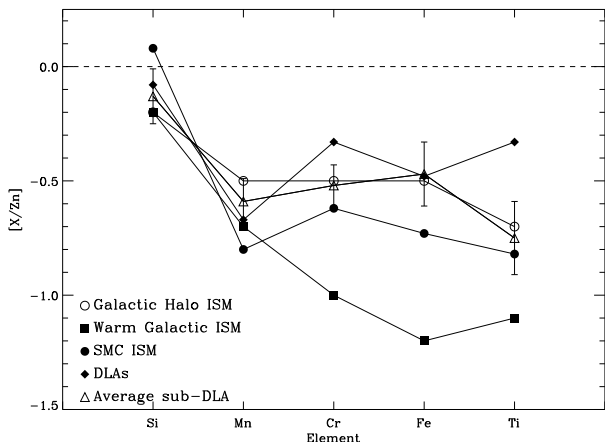


**Figure 10.** The abundances relative to Zn derived from the averaged sub-DLA spectra of the systems in this sample. Overplotted are the abundances of the Milky Way warm ISM, Milky Way halo, ISM abundances in the SMC, and DLA abundances.

The fraction of mass in metal ions in DLA systems compared to the critical density of the Universe is thus

$$\Omega_{met}^{DLA} = \frac{\rho_{met}}{\rho_{crit}} = \Omega_{HI}^{DLA} \cdot \bar{Z}_{DLA} \quad (8)$$

Péroux et al. (2005) measured  $\Omega_{HI}^{DLA}$  at  $z \sim 2.5$ , where the bulk of DLA metallicities are determined, to be  $\Omega_{HI}^{DLA} \sim 0.85 \times 10^{-3}$ . This then gives the comoving mass density of metals in DLAs to be  $\Omega_{met}^{DLA} \sim 2 \times 10^5 M_{\odot} \text{ Mpc}^{-3}$  (see also Kulkarni et al. 2007; Prochaska et al. 2006).

For sub-DLA systems, the ionisation fraction of the gas must be taken into account to determine the comoving mass density of metals contained in these systems. If we let  $y(N_{HI})$  be the neutral fraction of gas in sub-DLAs (which is a function of the neutral hydrogen column density as can be seen in Figure 4),  $f(N_{HI})$  the column density distribution in the sub-DLA regime, and the average metallicity  $\bar{Z}_{subDLA}$  we have then,

$$\Omega_m^{subDLA} = \frac{\mu H_0 m_H}{c \rho_{crit}} \int \frac{1}{y} \epsilon(Z) f(N_{HI}) \bar{Z}_{sub} N_{HI} dN_{HI} \quad (9)$$

where  $\epsilon(Z)$  is the ionisation correction term, which as can be seen from Figures 2 and 3 is a function of  $N_{HI}$  and the integral runs over the sub-DLA column density range of  $19.0 < \log N_{HI} < 20.3$ . We have used the ionization correction determined for Fe for the purpose of these calculations due to the better quality of atomic data for Fe.

Unfortunately, at lower redshifts the comoving gas density in sub-DLA systems is not well known, owing to the lack of space based UV surveys for H I at low  $z$ . Recently however, O’Meara et al. (2007) and also Péroux et al. (2005) determined the column density distribution function (CDDF) and comoving mass density of gas in sub-DLAs from observations with the Keck ESI, Magellan II MIKE spectrograph, and the VLT Kueyen UVES spectrograph. Combining the observations from both teams, we find that the CDDF is well fit by a power law ( $f(N_{HI}) = \beta N_{HI}^{\alpha}$ ) with  $\beta = 10^{4.84}$  and  $\alpha = -1.30$  in the sub-DLA regime of  $19.0 < \log N_{HI} < 20.3$ .

Survival analysis provides an estimate of the  $N_{HI}$ -weighted mean metallicities given in Table 3. Using these values for the column density distribution function and mean metallicities, Equation 9 can be integrated. As can be seen in Figures 6 and 7, the sub-DLA and DLA populations are dissimilar in their respective metallicities, sub-DLAs having a significantly higher  $N_{HI}$ -weighted mean metallicity of  $\langle [Zn/H]_{subDLA} \rangle \sim -0.08$  and  $\langle [Zn/H]_{DLA} \rangle \sim -0.8$  at  $z \lesssim 1$ . These calculations were carried out using three ionisation parameters and thus three separate levels of ionisation for these systems. We have used the results from the photoionisation models for Fe for the correction term  $\epsilon(N_{HI})_{FeII}$ , when evaluating Equation 9.

Results for the calculations of the comoving mass density of metals in the sub-DLAs are given in Table 3. The sub-DLAs thus appear to contain several times the comoving mass density of metals that the DLA systems contain at  $z < 1$ , and at least equal amounts at all redshifts. We stress however that the comoving mass density of H,  $\Omega_{HI}^{DLA}$ , is not well known at low  $z$  and warrants further investigation.

The more highly ionized phase of sub-DLAs has also been investigated as a possible location of the missing metals. At low density and temperatures  $T \sim 10^6$  K, the cooling time of the gas is roughly the age of the universe, so metal atoms can be essentially stuck in this hot phase. Fox et al. (2007) estimates that the metal content of the hot plasma in sub-DLAs at  $z \sim 2.5$  is roughly equal to the what we have determined here for the lower temperature gas in which Zn II arises.

## 9 DISCUSSION AND CONCLUSIONS

We have compiled all of the known Zn measurements in DLAs and sub-DLAs, and have examined  $\log N_{HI}$  vs.  $[Zn/H]$ . As has been reported in the past, the observed trend towards increasing metallicity with decreasing  $N_{HI}$  is again seen with the inclusion of these new data (Boisse et al. 1998; Khare et al. 2007; Meiring et al. 2006). We have used survival analysis to calculate a trend line to these data including the upper limits, which is determined to be of

Redshift Range	Metallicity Dex	$\Omega_Z^a$	$\rho_Z^a$ $M_\odot \text{ Mpc}^{-3}$
0.53 - 0.87	$+0.06 \pm 0.22$	$(7.8-31.3) \times 10^{-6}$	$(10.6-42.5) \times 10^5$
0.89 - 1.14	$-0.29 \pm 0.17$	$(3.5-13.9) \times 10^{-6}$	$(4.7-18.9) \times 10^5$
1.15 - 1.55	$-0.68 \pm 0.20$	$(1.4-5.7) \times 10^{-6}$	$(1.9-7.8) \times 10^5$
1.77 - 3.39	$-0.59 \pm 0.22$	$(1.8-7.0) \times 10^{-6}$	$(2.5-9.5) \times 10^5$

**Table 3.** The comoving mass density of metals,  $\Omega_{met}^{subDLA}$  and  $\rho_Z$  in sub-DLAs.

<sup>a</sup> Calculated based on the  $z \sim 2$  column density distribution

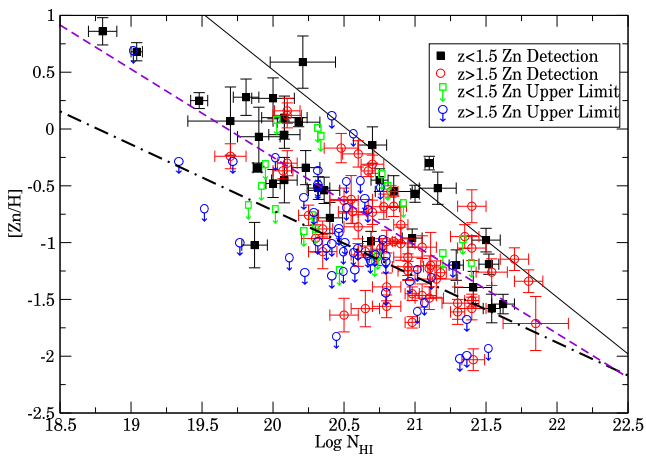


**Figure 11.**  $\text{Log } N_{\text{HI}}$  vs.  $[\text{Zn}/\text{H}]$  for all the systems given in Kulkarni et al. (2007), systems from this sample, and systems from Quast, Reimers & Baade (2008); Noterdaeme et al. (2008a); Prochaska et al. (2006); Dessauges-Zavadsky et al. (2003). The solid line is the ‘‘Obscuration Threshold’’ from Boisse et al. (1998), while the dashed line is the linear fit to these data ignoring the  $[\text{Zn}/\text{H}]$  upper limits, and the dashed-dotted line is the linear fit while including the upper limits.

the form  $[\text{Zn}/\text{H}] = -0.58N_{\text{HI}} + 10.9110$ . Without inclusion of the upper limits in the trend line, we determined  $[\text{Zn}/\text{H}] = -0.78N_{\text{HI}} + 15.27$ . Both Spearman and Kendall  $\tau$  tests independently determined that the probability of no correlation is  $p < 0.001$ , with the inclusion of the upper limits. A similar trend was seen in York et al. (2006) using composite spectra of a large number of SDSS QSO absorbers, and in Khare et al. (2007) using the literature data as well.

Interestingly, the amount of dust as estimated by  $[\text{Fe}/\text{Zn}]$  seems independent of  $N_{\text{HI}}$  in QSO absorbers over  $\sim 3$  decades in  $N_{\text{HI}}$  as is shown in Figure 12. Spearman and Kendall correlation tests each reveal a probability of no correlation of  $p \sim 84$  percent. The dust depletion on the other hand is known to correlate with the metallicity of the system as shown in Figure 13 where we show  $[\text{Fe}/\text{Zn}]$  vs  $[\text{Zn}/\text{H}]$  for QSO absorbers with both Fe and Zn detections (Kulkarni et al. 2007; Dessauges-Zavadsky et al. 2003; Quast, Reimers & Baade 2008; Noterdaeme et al. 2008a). Spearman and Kendall correlation tests show that the probability of no correlation between the metallicity and depletion as estimated by  $[\text{Fe}/\text{Zn}]$  to be  $p < 0.001$ .

The observed trend of increasing metallicity with decreasing  $N_{\text{HI}}$  seen in Fig. 11 contradicts measurements in

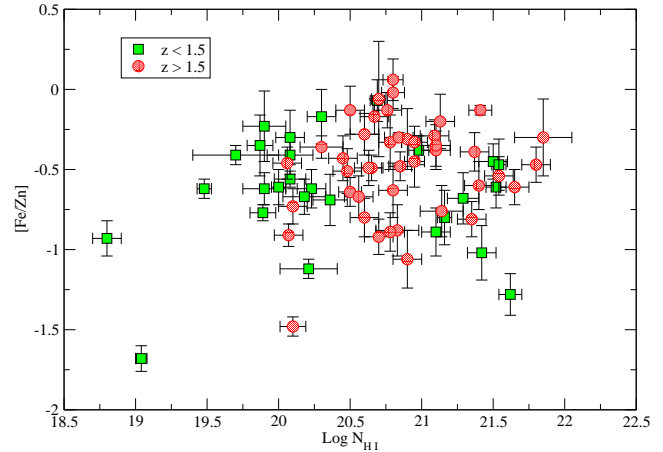


**Figure 12.**  $[\text{Fe}/\text{Zn}]$  vs.  $\text{Log } N_{\text{HI}}$  for QSO absorbers with both Fe and Zn detections from this work, as well as systems from Kulkarni et al. (2007); Dessauges-Zavadsky et al. (2003); Prochaska et al. (2006); Quast, Reimers & Baade (2008); Noterdaeme et al. (2008a).

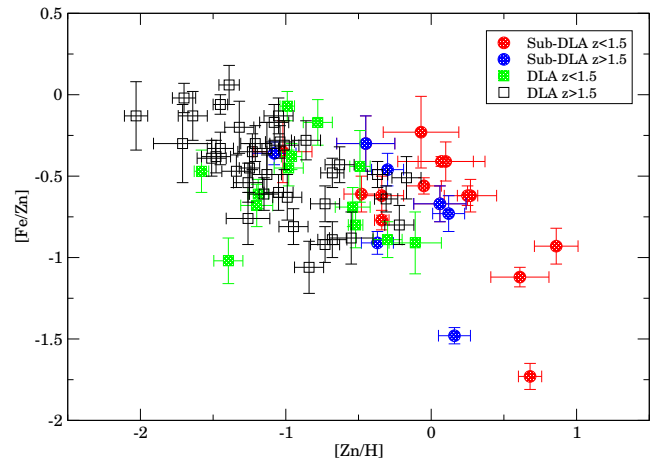


**Figure 13.**  $[\text{Fe}/\text{Zn}]$  vs.  $[\text{Zn}/\text{H}]$  for QSO absorbers with both Fe and Zn detections from this work, as well as systems from Kulkarni et al. (2007); Dessauges-Zavadsky et al. (2003); Prochaska et al. (2006); Quast, Reimers & Baade (2008); Noterdaeme et al. (2008b).

the local ISM of the Milky Way and the Magellanic Clouds, where different lines of sight show roughly solar metallicity gas although the sightlines may contain a range of  $N_{\text{HI}}$  values. Abundance gradients could not produce the effect as is seen; if the majority of DLAs are produced in the outskirts of the disks of massive spirals where the abundances would be lower due to the gradient, a simultaneous gradient of decreasing  $N_{\text{HI}}$  with decreasing galactic radius which is not observed would be necessary to explain the lower  $N_{\text{HI}}$  systems with higher abundances.

In all likelihood, the sightlines through DLAs and sub-DLAs pass through gas rich galaxies of a wide range of morphologies and masses. The fact that the ionization fractions in sub-DLAs from the models above as well as in Péroux et al. (2007) show a range of values for a given  $N_{\text{HI}}$ , as well as the fact that not all sub-DLAs are metal rich sug-

gest that this is indeed the case. There are however several lines of evidence to suggest that DLAs are mainly sampling low mass gas rich dwarf galaxies such as the SMC:

- The abundances in DLA systems are low ( $[Zn/H] \sim -0.8$ ) and slowly evolving, which is consistent with the observations and chemical evolution models of local dwarf galaxies. The  $N_{HI}$ -weighted mean metallicity of DLAs does not track the global chemical evolution models and is essentially flat for  $1 < z < 3$ , which is predicted by Pagel & Tautvaišienė (1998) for the SMC.

- The molecular fraction of gas in DLAs is small Ledoux, Petitjean, & Srianand (2003), consistent with CO surveys of local dwarf galaxies (Leroy et al. 2005). The molecular fraction in dwarf galaxies is substantially smaller than in more massive systems (Leroy et al. 2005), consistent with FUV stellar observations in the Magellanic Clouds (e.g. Tumlinson et al. 2002). Although  $H_2$  was detected in most of the SMC sight lines from Tumlinson et al. (2002), the molecular content of the SMC was likely much lower in the past as there was a long quiescent period in the star formation history of the SMC. The molecular content of sub-DLAs has not been investigated as thoroughly, however molecule rich sub-DLAs have been observed (Quast, Reimers & Baade 2008; Noterdaeme et al. 2008a).

- Followup imaging studies of DLAs show that the majority of the galaxies associated with the DLA absorption, when detected have  $L < L_*$  (Le Brun et al. 1997; Rao et al. 2003; Kulkarni et al. 2006). The low mass local dwarf galaxies observed in Geha et al. (2006) were determined to have total baryonic masses actually dominated by the gas, and not the stellar content, with gas fractions as high as  $f_{gas} = 95\%$  and  $\langle f_{gas} \rangle \sim 0.6$ . This could explain the low luminosities observed in DLA galaxies, and the low detection rate in followup imaging.

This still raises the question as to *why* we do not see metal rich DLAs and do see more metal rich systems at lower  $N_{HI}$ , and the observed relationship between  $[Zn/H]$  and  $N_{HI}$ . One proposed explanation is that there is a selection effect causing the higher metallicity DLAs to be systematically undersampled due to dust obscuring the background QSO to magnitudes fainter than what is observable with the current classes of instrumentation (Lauroesch et al. 1996; Boisse et al. 1998; Vladilo & Péroux 2005). The amounts of dust in QSO absorbers as estimated by ratios of volatile and refractory elements such as  $[Cr/Zn]$  or  $[Fe/Zn]$  is strongly correlated with the systems metallicity (Meiring et al. 2006) the higher metallicity systems thus contain more dust and could be obscuring the background QSO.

The amount of extinction need not be very large to exclude a large number of background QSOs from being observed. In fact, as can be seen in Figure 14, only  $\sim 4$  percent of SDSS DR7 QSOs have  $m_{g'} < 18.0$  at  $1.25 < z_{em} < 3.5$ , so even with a modest 0.5 magnitudes of extinction (less than 50 percent of the estimated extinction amounts in Vladilo & Péroux (2005) for a solar metallicity DLA) we would be left with only 4 percent of QSOs bright enough to observe. As we are currently magnitude limited at  $m_g \lesssim 18.5$  with current instrumentation, a large number of DLAs could be lying unobserved in front of fainter QSOs.

If this is indeed true, then one would expect that the *observed* DLAs would have properties more similar to dwarf

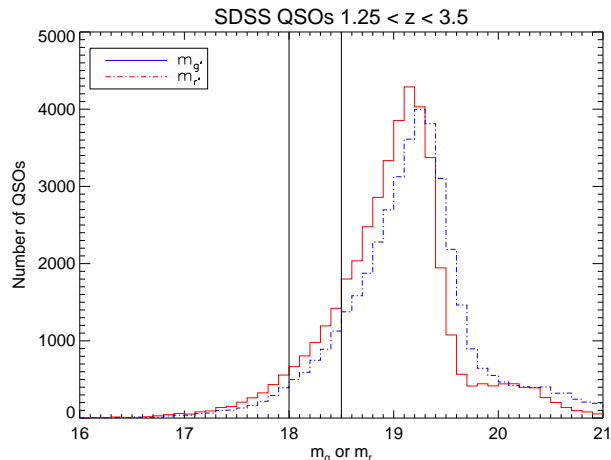


**Figure 14.** The distribution of SDSS  $g'$  and  $r'$  magnitudes of QSOs with  $1.25 < z < 3.5$ . The vertical lines at  $m = 18.0$  and  $m = 18.5$  represent the approximate magnitude limitations of the current instrumentation with and without an extinction effect respectively.

or SMC type galaxies. The DLAs do seem to exhibit a more gradual chemical evolution similar to the SMC, as seen in Figures 6 and 7, and the molecular content along with the low luminosities of DLA host galaxies observed in imaging support the claim, as highlighted in the list above. With lower  $N_{HI}$  and thus likely lower levels of extinction, the sub-DLAs are less affected by the dust extinction bias than the more  $H I$  rich traditional DLAs (Lauroesch et al. 1996). This could possibly explain why the mean abundances in these sub-DLA systems are significantly higher than their DLA counterparts. An alternative explanation has been put forward by Khare et al. (2007), who suggest that based on the observed mass metallicity relationship of Tremonti et al. (2004) these higher metallicity sub-DLAs may arise in more massive spiral galaxies while the lower metallicity DLAs would be more similar to gas rich dwarfs.

More work still is needed in several areas though. More space based observations are necessary to constrain the low redshift column density distribution of sub-DLA systems, and hence  $\Omega_{HI}^{subDLA}$  which is currently poorly understood. If  $\Omega_{HI}^{subDLA}$  has varied from  $z \sim 2.5$  to  $z \sim 1.0$ , the contribution of these sub-DLAs to the metal budget will alter accordingly.

The Lyman limit systems with  $17.2 < \log N_{HI} \lesssim 19.0$  are yet another possible reservoir of metals that have been hitherto understudied, although progress is being made (see for instance Charlton et al. 2003; Misawa, Charlton & Narayanan 2008). Several difficulties arise in these systems as  $N_{HI}$  cannot be constrained due to the lack of damping wings in the Lyman- $\alpha$  profile in this column density range, and with such low neutral hydrogen column densities the effects of ionization are likely to be much more important. Nonetheless, this is certainly an area worth investigation.

The ionisation levels in sub-DLAs are still not particularly well known, which is why we have presented a broad range of cases to illustrate the range of possible values in determining  $\Omega_{met}$  and  $\rho_Z$ . With further UV spectra of sub-DLAs, the higher ionization lines of S III, Si III, Fe III could be accessed, providing further constraints on the levels of

ionization in the gas. The Si III/Si II ratio seems to be a promising ionization indicator, as the ratio increases faster than other adjacent ion ratios such as Fe III/Fe II, enabling tighter constraints to be placed on the ionization parameter. Simultaneously, the H<sub>2</sub> transitions could also be observed to determine the molecular content in these systems.

This series of papers has roughly doubled the total number of sub-DLA observations, and nearly quadrupled the sample at  $z < 1.5$ , and done so with quality high resolution spectra. Complementary to studying these galaxies in absorption, the typically more difficult task of imaging these galaxies still needs to be undertaken. Deep imaging in multiple bands ( $g'$ ,  $r'$ ,  $i'$ ,  $K$ ) of sub-DLAs is necessary to determine the stellar content of these systems. Almost certainly, the sightlines that produce sub-DLAs are sampling a variety of morphological types of gas rich galaxies. The systems with high metallicity and higher velocity widths may however be more representative of massive spiral galaxies.

## ACKNOWLEDGMENTS

We thank the exceptionally helpful staff of Las Campanas Observatory for their assistance during the observing runs. We would also like to thank the anonymous referee for their helpful suggestions which greatly improved the presentation and substance. J. Meiring and V.P. Kulkarni gratefully acknowledge support from the National Science Foundation grant AST-0607739 (PI Kulkarni). J. Meiring acknowledges partial support from a South Carolina Space Grant graduate student fellowship for a portion of this work.

## REFERENCES

- Adelberger K.L., Steidel C.C., Shapley A.E., Hunt M.P., Erb D.K., Reddy N.A., Pettini M., 2004, *ApJ*, 607, 226
- Bernstein R., Schectman S.A., Gunnels S., Mochnicki S., Athey A., 2003 *SPIE*, 4841, 1694
- Boisse P., Le Brun V., Bergeron J., Deharveng J., 1998, *A&A*, 333, 841
- Bouche N., Murphy M.T., Péroux C., Csabai I., Wild V., 2006, *MNRAS*, 371, 495
- Bouche N., Lehnert M.D., Proux C., 2006, *MNRAS*, 367, 16
- Bouche N., Lehnert M.D., Aguirre A., Proux C., Bergeron J., 2008, *MNRAS*, 378, 525
- Bowen D.V., Tripp T.M., Jenkins E.B., 2001, *AJ*, 121 1456
- Cen R., Ostriker J.P., Prochaska J.X., Wolfe A.M., 2003, *ApJ*, 598, 741
- Charlton J.C., Ding J., Zonak S.G., Churchill C.W., Bond N.A., Rigby J.R., 2003, *ApJ*, 589, 111
- Chen H.W., Lanzetta K.M., 2003, *ApJ*, 597, 706
- Danforth C.W., Shull M.J., 2008, *ApJ*, 679, 194
- Dessauges-Zavadsky M., Prochaska J.X., D'Odorico S., 2002, *A&A*, 391, 801
- Dessauges-Zavadsky M., Péroux C., Kim T.S., D'Odorico S., McMahon R.G., 2003, *MNRAS*, 345, 447
- Dessauges-Zavadsky M., Ellison S.L., Murphy M.T., 2009, *MNRAS*, in press (arXiv:0904.2531)
- Ding J., Charlton J.C., Churchill C.W., Palma C., 2003, *ApJ*, 590, 746
- D'Odorico S., Cristiani S., Dekker H., Hill V., Kaufer A., Kim T., Primas F., 2000, *SPIE*, 4005, 121
- Ellison, S., 2006, *MNRAS*, 368, 355
- Feigelson E.D., Nelson P.I., 1985, *ApJ*, 293, 192
- Ferland G. J., Korista K.T., Verner D.A., Ferguson J.W., Kingdon J.B., Verner E.M., 1998, *PASP*, 110, 761
- Ferrara A., Scannapieco E., Bergeron J., 2005, *ApJ*, 634, L37
- Fox A.J., Petitjean P. Ledoux C. Srianand R., 2007, *ApJ*, 668, L15
- Frank S., Mathur S., York D.G., 2008, *AJ*, submitted
- Gharanfoli S., Kulkarni V.P., Chun M.R., Takamiya M., 2007, *ApJ*, 133, 130
- Geha M., Blanton M.R., Masjedi M., West A.A., 2006, *ApJ*, 643, 240
- Gilmore G., 2001, *ASPC*, 230, 3
- Gratton R.G., Caretta E., Claudi R., Lucatello S., Barbieri M., 2004, *A&A*, 404, 187
- Haardt F., Madau P., 1996, *ApJ*, 461, 20
- Harris J., Zaritsky D., 2004, *ApJ*, 127, 1531
- Herbert-Fort S., Prochaska J.X., Dessauges-Zavadsky M., Ellison S.L., Howk J.C., Wolfe A.M., Prochter G.E., 2006, *PASP*, 118, 1077
- Hopkins A.M., Rao S.M., Turnshek D.A., 2005, *ApJ*, 630, 108
- Howk J.C., Sembach K.R., 1999, *ApJ*, 523, L141
- Kaplan E.L., Meier P., 1958, *JASA*, 53, 282
- Khare P., Kulkarni V.P., Lauroesch J.T., York D.G., Crotts P.S., Nakamura O., 2004, *ApJ*, 616, 86
- Khare P., Kulkarni V.P., Péroux C., York D.G., Lauroesch J.T., Meiring J.D., 2007, *A&A*, 464, 487
- Kulkarni V.P., Fall S.M., Lauroesch J.T., York D.G., Welty D.E., Khare P., Truran J.W., 2005, *ApJ*, 618, 68
- Kulkarni V.P., Woodgate B.E., York D.G., Thatte D.G., Meiring J., Palunas P., Wassell E., 2006, *ApJ*, 636, 30
- Kulkarni V.P., Khare P., Péroux C., York D.G., Lauroesch J.T., Meiring J.D., 2007, *ApJ*, 661, 88
- Lauroesch J.T., Truran J.W., Welty D.E., York D.G., 1996, *PASP*, 108, 641
- Le Brun V., Bergeron J., Boisse P., Deharveng J.M., 1997, *A&A*, 321, 733
- Ledoux C., Bergeron J., Petitjean P., 2002, *A&A*, 385, 802
- Ledoux C., Petitjean P., Srianand R., 2003, *MNRAS*, 346, 209
- Ledoux, C. Petitjean, P., Moller, P., Fynbo, J., Srianand R., 2006, *A&A*, 457, 71
- Lehner N., Savage B.D., Richter P., Sembach K., Tripp T.M., Wakker B.P., 2007, *ApJ*, 658, 680
- Leroy A., Bolatto A.D., Simon J.D., Blitz L., 2005, *ApJ*, 625, 763
- Lodders, K., 2003, *ApJ*, 591, 1220
- Madau P., Haardt F., Rees M.J., 1999, *ApJ*, 514, 648
- Masiero J.R., Charlton J.C., Ding J., Churchill C.W., Kacprzak G., 2005, *ApJ*, 623, 57
- Meiring J.D., Kulkarni V.P., Khare P., Bechtold J., York D.G., Cui J., Lauroesch J.T., Crotts A.P.S., Nakamura O., 2006, *MNRAS*, 370, 43
- Meiring J.D., Lauroesch J.T., Kulkarni V.P., Péroux C., Khare P., York D.G., Crotts A.P.S., 2007, *MNRAS*, 376, 557
- Meiring J.D., Kulkarni V.P., Lauroesch J.T., Péroux C., Khare P., York D.G., Crotts A.P.S., 2008, *MNRAS*, 384,

1015  
 Meiring J.D., Kulkarni V.P., Lauroesch J.T., Péroux C., Khare P., York D.G., 2008, MNRAS, 393, 1513  
 Misawa T., Charlton J.C., Narayanan A., 2008, ApJ, 679, 220  
 Mishenina T.V., Kovtyukh V.V., Soubiran C., Travaglio C., Busso M., 2002, A&A, 396, 189  
 Morton D.C., 2003, ApJS, 149, 205  
 Nissen P.E., Chen Y.Q., Schuster W.J., Zhao G., 2000, A&A, 353, 722  
 Nissen P. E., Chen Y. Q., Asplund M., Pettini M., 2004, A&A, 415, 993  
 Noterdaeme P., Petitjean P., Ledoux C., Srianand R., Ivanachik A., 2008, A&A, 491, 397  
 Noterdaeme P., Ledoux C., Petitjean P., Srianand R., 2008, A&A, 481, 327  
 O’Meara J.M., Prochaska J.X., Burles S., Prochter G., Bernstein R.A., Burgess K., 2007, ApJ, 656, 666  
 Pagel B.E.J., Tautvaisiene G., 1998, MNRAS, 299, 535  
 Péroux C., Storrie-Lombardi L., McMahon R., Irwin M., & Hook I., 2001, AJ, 121, 1799  
 Péroux C., Dessauges-Zavadsky M., D’Odorico S., Kim T.S., McMahon R., 2003, MNRAS, 345, 480  
 Péroux C., McMahon R.G., Storrie-Lombardi L.J., Irwin M.J., 2003, MNRAS, 346, 1103  
 Péroux C., Dessauges-Zavadsky M., D’Odorico S., Kim T.S., McMahon R.G., MNRAS, 363, 479  
 Péroux C., Kulkarni V.P., Meiring J., Ferlet R., Khare P., Lauroesch J.T., Vladilo G., York D.G., 2006, A&A, 450, 53  
 Péroux C., Meiring J., Kulkarni V.P., Ferlet R., Khare P., Lauroesch J.T., Vladilo G., York D.G., 2006, MNRAS, 372, 369  
 Péroux C., Dessauges-Zavadsky M., D’Odorico S., Kim T.S., McMahon R.G., MNRAS, 2007, 382, 177  
 Péroux C., Meiring J.D., Kulkarni V.P., Khare P., Lauroesch J.T., Vladilo G., York D.G., 2008, MNRAS, 386, 2209  
 Pettini M., Ellison S.L., Steidel C.C., Bowen, D.V., 1999, ApJ, 510, 576  
 Pettini M., Ellison S.L., Steidel C.C., Shapley A.E., Bowen, D.V., 2000, ApJ, 532, 65  
 Pei Y., Fall S.M., Hauser M.G., 1995, ApJ, 522, 604  
 Prochaska J.X., Wolfe A.M., 1999, ApJS, 121, 369  
 Prochaska J.X., Wolfe A.M., 2002, ApJ, 566, 68  
 Prochaska J.X., Gawiser E., Wolfe A.M., Castro S., Djorgovski S. G., 2003, ApJ, 595, L9  
 Prochaska J.X., Howk J.C., O’Meara J.M., Tytler D., Wolfe A.M., Kirkman D., Lubin D., Suzuki N., 2002, ApJ, 571, 693  
 Prochaska J.X., O’Meara J.M., Herbert-Fort S., Burles S., Prochter G.E., Bernstein R.A., 2006, ApJL, 648, 97  
 Quast R., Reimers D., Baade R., 2008, A&A, 477, 443  
 Rao S.M., Nestor D.B., Turnshek D.A., Lane W.M., Monier E.M., Bergeron J., 2003, ApJ, 595, 94  
 Rao S.M., Turnshek D.A., Nestor D.B., 2006, ApJ, 636, 610  
 Richards G.T., Fan X., Schneider D.P., Vanden Berk D.E., Strauss M.A., York D.G., Anderson J.E., Anderson S.F., 2001, AJ, 121, 2308  
 Rocha-Pinto H.J., Scalo J., Maciel W. J., Flynn C., 2000, A&A, 358, 869  
 Samland M., 1998, ApJ, 496, 155  
 Savage B.D., Sembach K.R., 1996, ApJ, 379, 245  
 Savaglio, S. et al. 2005, ApJ, 635, 260  
 Searle L., Sargent W. L. W., 1972, ApJ, 173, 25  
 Srianand R., Noterdaeme P., Ledoux C., Petitjean P., 2008, A&A, 482, 39  
 Tremonti C. A. et al. 2004, ApJ, 613, 898  
 Tripp T.M., Sembach K.R., Bowen D., Savage B.D., Jenkins E.B., Lehner N., Richter P., 2008, ApJ, 177, 39  
 Tumlinson J., Shull J. M., Rachford B.L., Browning M.K., Snow T.P., Fullerton A.W., Jenkins E.B., Savage B.D., Crowther P.A., Moos H.W., et al., 2002, ApJ, 566, 857  
 Vladilo G., Centurión M., Bonifacio P., Howk C., 2001, ApJ, 557, 1007  
 Vladilo G., Péroux C., 2005, A&A, 444, 461  
 Vidal-Madjar A., Laurent C., Bonnet R. M., York D. G., 1977, ApJ, 211, 91  
 Welty D.E., Hobbs L.M., York D.G., 1991, ApJS, 75, 425  
 Welty D. E., Lauroesch J.T., Blades J.C., Hobbs L.M., York, D.G., 1997, ApJ, 489, 672  
 Welty D.E., Hobbs L.M., Lauroesch J.T., Morton D.C., Spitzer L., York D.G., 1999, ApJS, 124, 465  
 Wolfe A.M., Prochaska J.X., 2000, ApJ, 545, 591  
 Wolfe A.M., Gawiser E., Prochaska J.X., 2005, ARAA, 43, 1, 861  
 York, D.G., Adelman, J., Anderson, J.E., et al. 2000, AJ, 120, 1579  
 York D.G., Khare P., Vanden Berk D., Kulkarni V.P., Crofts A.P.S., Lauroesch J.T., Richards G.T., et al., 2006, MNRAS, 367, 945  
 Zwaan M.A., van der Hulst J.M., Briggs F.H., Verheijen M.A.W., Ryan-Weber E.V., 2005, MNRAS, 364, 1467  
 Zwaan M.A., Walter F., Ryan-Weber E., Brinks E., de Blok W.J.G., Kennicutt R.C., 2008, AJ, in press

This paper has been typeset from a  $\text{\TeX}$ / $\text{\LaTeX}$  file prepared by the author.